

GRB 000418: A Hidden Jet Revealed?

E. Berger¹, A. Diercks¹, D. A. Frail², S. R. Kulkarni¹, J. S. Bloom¹, R. Sari³, J. Halpern⁴, N. Mirabal⁴, G. B. Taylor³, K. Hurley⁵, G. Pooley⁶, K. M. Becker⁷, R. M. Wagner⁸, D. M. Terndrup⁸, T. Statler⁹, E. Mazets¹⁰, T. Cline¹¹

ABSTRACT

We report on optical, near-infrared and centimeter radio observations of GRB 000418 which allow us to follow the evolution of the afterglow from 2 to 200 days after the γ -ray burst. In modeling these broad-band data, we find that an isotropic explosion in a constant density medium is unable to simultaneously fit both the radio and optical data. However, a jet-like outflow with an opening angle of 10-20° provides a good description of the data. The evidence in favor of a jet interpretation is based on the behavior of the radio light curves, since the expected jet break is masked at optical wavelengths by the light of the host galaxy. We also find evidence for extinction, presumably arising from within the host galaxy, with $A_V^{host}=0.4$ mag, and host flux densities of $F_R = 1.1 \mu\text{Jy}$ and $F_K = 1.7 \mu\text{Jy}$. These values supercede previous work on this burst due to the availability of a broad-band data set allowing a global fitting approach. A model in which the GRB explodes into a wind-stratified circumburst medium cannot be ruled out by these data. However, in examining a sample of other bursts (e.g. GRB 990510, GRB 000301C) we favor the jet interpretation for GRB 000418.

¹California Institute of Technology, Palomar Observatory 105-24, Pasadena, CA 91125

²National Radio Astronomy Observatory, P. O. Box O, Socorro, NM 87801

³California Institute of Technology, Theoretical Astrophysics 103-33, Pasadena, CA 91125

⁴Astronomy Department, Columbia University 550 West 120th St., New York, NY 10027

⁵University of California, Berkeley, Space Sciences Laboratory, Berkeley, CA 94720-7450

⁶Mullard Radio Astronomy Observatory, Cavendish Laboratory, Madingley Road, Cambridge CB3 0HE

⁷Department of Physics, Oberlin College Oberlin, OH 44074

⁸Ohio State University, Department of Astronomy, Columbus, OH, 43210

⁹Ohio University, Department of Physics and Astronomy, Athens, OH, 45701

¹⁰Ioffe Physico-Technical Institute, St. Petersburg, 194021 Russia

¹¹NASA Goddard Space Flight Center, Code 661, Greenbelt, MD 20771

Subject headings: gamma rays: bursts – radio continuum: general – optical continuum: general

1. Introduction

GRB 000418 was detected on April 18, 2000, at 09:53:10 UT by the *Ulysses*, *KONUS-Wind* and *NEAR* spacecraft, which are part of the third interplanetary network (IPN). The event lasted ~ 30 s, and a re-analysis of the early *Ulysses* data (Hurley, Cline & Mazets 2000) gives a fluence of 4.7×10^{-6} erg cm $^{-2}$ in the 25-100 keV band. A fit to the total photon spectrum from the *KONUS* data 2×10^{-5} erg cm $^{-2}$ in the energy range 15 - 1000 keV. Intersecting IPN annuli resulted in a 35 arcmin 2 error box, in which Klose *et al.* (2000b) identified a variable near-infrared (NIR) source. The early R-band light curve of this source was described by Mirabal *et al.* (2000) as having a power-law decay $t^{-0.84}$, typical for optical afterglows. The redshift for the host galaxy of $z \simeq 1.119$ was measured by Bloom *et al.* (2000) from an [OII] emission line doublet. Assuming cosmological parameters of $\Omega_M=0.3$, $\Lambda_0=0.7$ and $H_0=65$ km s $^{-1}$ Mpc $^{-1}$, this redshift corresponds to a luminosity distance $d_L = 2.5 \times 10^{28}$ cm and gives an implied isotropic γ -ray energy release of $E_\gamma = 1.7 \times 10^{52}$ erg.

Klose *et al.* (2000b) have recently summarized optical/NIR data observations of GRB 000418. In this paper we present additional optical/NIR data and a complete set of radio observations between 1.4 GHz and 22 GHz, from 10 to 200 days after the burst. We use this broad band data set to fit several models, deriving the physical parameters of the system.

2. Observations

2.1. Optical Observations

In Table 1 we present deep optical photometry obtained at Palomar, Keck¹², and MDM observatories covering six weeks following the GRB as well as data from the extant

¹²The W. M. Keck Observatory is operated by the California Association for Research in Astronomy, a scientific partnership among California Institute of Technology, the University of California and the National Aeronautics and Space Administration.

literature.

All of the optical data was overscan corrected, flat-fielded, and combined in the usual manner using IRAF (Tody 1993). PSF-fitting photometry was performed relative to several local comparison stars measured by Henden (2000) using DoPhot (Schechter, Mateo & Saha 1993). Short exposures of the field in each band were used to transfer the photometry (Henden 2000) to several fainter stars in the field. Several of the Keck+ESI measurements, and the Palomar 200" measurement were made in Gunn-r and Gunn-i respectively and were calibrated by transforming the local comparison stars to the Gunn system using standard transformations (Wade *et al.* 1979, Jorgensen 1994). We add an additional 5% uncertainty in quadrature with the statistical uncertainties to reflected the inherent imprecision in these transformations.

The Ks-band image of the field was obtained on the Keck I Telescope on Manua Kea, Hawaii with the Near Infrared Camera. We obtained a total of 63 one-minute exposures which we reduced and combined with the IRAF/DIMSUM package modified by D. Kaplan. There was significant cloud and cirrus cover and so the night was not photometric.

The HST STIS/Clear image was obtained on 4 June 2000 UT as part of the TOO program # 8189 (P.I. A. Fruchter) and made public on 2 September 2000 UT. Five images of 500 s each were obtained which we combined using the IRAF/DITHER task. The final plate scale is 25 milliarcsec pixel⁻¹.

We corrected all optical measurements in Table 1 for a Galactic foreground reddening of $E(B - V) = 0.032$ (Schlegel, Finkbeiner & Davis 1998) at the position of the burst $(l, b) = (261.16, 80.78)$ before converting to flux units (Fukugita, Shimasaku & Ichikawa 1995, Bessell & Brett 1988) assuming $R_V=3.1$.

2.2. Radio Observations

Radio observations were undertaken at a frequency of 15 GHz with the Ryle Telescope. All other frequencies were observed with either the NRAO¹³ Very Large Array (VLA) or the Very Long Baseline Array (VLBA). A log of these observations can be found in Table 2. The data acquisition and calibration for the Ryle and the VLA were straightforward (see Frail *et al.* 2000a for details).

¹³The NRAO is a facility of the National Science Foundation operated under cooperative agreement by Associated Universities, Inc. NRAO operates the VLA and the VLBA

The single VLBA observation was carried out at 8.35 GHz with a total bandwidth of 64 MHz in a single polarization using 2 bit sampling for additional sensitivity. The nearby ($<1.3^\circ$) calibrator J1224+2122 was observed every 3 minutes for delay, rate and phase calibration. Amplitude calibration was obtained by measurements of the system temperature in the standard way. The coordinates for GRB 000418 derived from the VLBA detection are (epoch J2000) $\alpha = 12^h 25^m 19.2840^s$ ($\pm 0.015^s$) $\delta = +20^\circ 06' 11.141''$ ($\pm 0.001''$).

3. The Optical Light Curve and Host Galaxy

In Figure 1 we display the R and K-band light curves constructed from measurements in Table 1. The pronounced flattening of the R-band light curve at late times is reasonably attributed to the optical afterglow fading below the brightness of the underlying host galaxy. A noise-weighted least squares fit was made to the data of the form $f_R = f_o t_o^\alpha + f_{host}$ for which we derive $f_o = 23.4 \pm 2.1 \mu\text{Jy}$, $\alpha_o = -1.41 \pm 0.08$ and $f_{host} = 1.08 \pm 0.06 \mu\text{Jy}$ with a reduced $\chi_r^2 = 0.94$. Our inferred R-band magnitude for the host galaxy $R_{host} = 23.66 \pm 0.06$ is nearly identical to that obtained from a similar analysis by Klose *et al.* (2000b). In order to estimate the effect of the host in other optical bands we scaled R_{host} for GRB 000418 to a spectrum of the host galaxy of GRB 980703 (Bloom *et al.* 1998) ($z = 0.966$) whose magnitude was measured in seven broad-band colors (B, V, R, I, J, H, and K). Our results indicate that 50-100% of the flux in some bands is due to the host galaxy after the first 10 days. Therefore, for the afterglow modeling in §5 we chose not to include the late-time measurements of GRB 000418 in the B, V, and Gunn-i bands.

4. The Radio Light Curves

In Figure 1 we display the radio light curves at 4.86, 8.46, 15 and 22 GHz. To first order all four frequencies show a maximum near 1 mJy on a time scale of 10 to 20 days. There is no discernible rising trend at any frequency. This is most clear at 8.46 GHz, where beginning 10 days after the burst, the light curve undergoes a steady decline, fading from 1 mJy to 0.1 mJy over a six month period. The temporal slope of the 8.46 GHz light curve after the first two months $\alpha_{rad} = -1.37 \pm 0.10$ ($\chi_r^2 = 1.4$) is similar to the optical R-band curve $\alpha_{opt} = -1.41 \pm 0.08$.

Superimposed on this secular decrease, there exist point-to-point variability of order 50%, especially in the early measurements. We attribute these variations to interstellar scintillation (ISS) (Goodman 1997, Walker 1998). The method by which we estimate the

magnitude of the intensity fluctuations induced by ISS as a function of frequency and time is described in full by Berger *et al.* (2000). Briefly, we estimate the magnitude of scattering with the model of Taylor & Cordes (1993), and use this to calculate the transition frequency ν_0 between weak and strong scattering using Walker (1997). The normalizations used in Goodman (1997) give slightly larger values of ν_0 .

In the direction toward GRB 000418 we derive $\nu_0 \simeq 3.6$ GHz and therefore most of our measurements were taken in the weak ISS regime. In this case the modulation scales as $\nu^{-17/12}$, with a maximum of 65% expected at 4.86 GHz and 30% at 8.46 GHz. At 15 GHz and 22 GHz we estimate that the ISS-induced fluctuations are only a fraction of the instrumental noise. The expansion of the fireball will eventually quench ISS when the angular size of the fireball exceeds the angular size of the first Fresnel zone at the distance of the scattering screen. The fireball size, and hence the quenching timescale, is model-dependent, and we use the derived total energy and density from the global fits (see §5 below) to estimate this time for each model. For example, in a simple spherical fireball this occurs after 15 days at 4.86 GHz and 10 days at 8.46 GHz, and thereafter the modulation indices decline as $t^{-35/48}$. We note that the observed fluctuations at 4.86 and 8.46 GHz conform to the predicted level of ISS, but that the measurements at 8.46 GHz from around 50 days after the burst deviate by a factor of three from the predicted ISS level.

In addition, we use the scintillation pattern to estimate the true χ_r^2 for each model, by adding in quadrature to the instrumental noise an additional ISS-induced uncertainty, $\sigma_{\text{ISS}} = m_p F_{\nu, \text{model}}$, where m_p and $F_{\nu, \text{model}}$ are the modulation index and model flux density at frequency ν , respectively (Berger *et al.* 2000).

5. Global Model Fits

The optical and radio data presented here have allowed us to track the evolution of the GRB 000418 afterglow from 2 to 200 days after the burst. With careful modeling of the light curves, it should be possible to infer the physical parameters of the blast wave and thereby gain some insight into the nature of GRB progenitors. In particular, the hydrodynamic evolution of the shock is governed by the energy of the explosion, the geometry of the expanding ejecta shock and the type of environment into which the GRB explodes (Sari, Piran & Narayan 1998, Wijers & Galama 1999, Chevalier & Li 1999, Panaitescu & Kumar 2000a). We will consider three basic models: a spherical explosion in a constant density medium, collimated ejecta (*i.e.*, jets) interacting with a constant density medium, and a spherical explosion in a wind-blown medium.

The starting point for any afterglow interpretation is the cosmological fireball model (e.g. Mészáros & Rees 1997, Waxman 1997). A point explosion of energy E_0 expands relativistically into the surrounding medium (with density $\rho \propto r^{-s}$, where $s = 0$ for constant density ISM and $s = 2$ for a wind) and the shock produced as a result of this interaction is a site for particle acceleration. The distribution of electrons is assumed to be a power-law of index p , and the fraction of the shock energy available for the electrons and the magnetic field is ϵ_e and ϵ_B , respectively. The values of these three quantities (p , ϵ_e and ϵ_B) are determined by the physics of the shock and the process of particle acceleration and in the absence of detailed understanding are taken to be constant with time.

The instantaneous broad-band synchrotron spectrum can be uniquely specified by the three characteristic frequencies ν_a , ν_m , and ν_c (*i.e.*, synchrotron self-absorption, synchrotron peak, and cooling), the peak flux density f_m , and p . For this work we adopt the smooth spectral shape as given by Granot *et al.* (1999a, 1999b) rather than the piecewise, broken power-law spectrum used by other authors (*e.g.*, Wijers & Galama 1999). The evolution of the spectrum (and thus the time dependence of ν_a , ν_m , ν_c and f_m) is governed by the geometry of the explosion (spherical or a collimated into a jet-like outflow), and the properties of the external environment (constant density or a radial density profile). Our approach is to adopt a model (sphere, wind, jet, etc.) and solve for the above spectral parameters using the entire optical and radio data set. The advantages and details of global model fitting are discussed by Berger *et al.* (2000).

The simplest model is a spherically symmetric explosion in a constant density medium (*ISM*: Sari *et al.* 1998). The total χ_r^2 for this model (see Table 3) gives a highly unsatisfactory fit to the data. On close inspection (Figure 1) we find that the model systematically underpredicts the optical flux. Adding extinction from the host galaxy only makes this worse. The fundamental difficulty with the *ISM* model is that it predicts $f_m = \text{constant}$, independent of frequency. In this case, since it is the radio data that is responsible for defining the peak of spectrum, it results in a value of f_m that is too low at higher frequencies.

To obtain better fits to the joint optical and radio data sets we look to models for which f_m is time-dependent. One such model is a collimated outflow into a medium with uniform density (*Jet*: Rhoads 1997, Rhoads 1999, Sari, Piran & Halpern 1999). The clearest observational signature of the *Jet* model is an achromatic break in the light curves at t_j (*e.g.*, Harrison *et al.* 1999). At radio wavelengths (*i.e.*, below ν_m) at t_j we expect a transition from a rising $t^{1/2}$ light curve to a shallow decay of $t^{-1/3}$, while at optical wavelengths the decay is expected to steepen to t^{-p} . These decay indices refer to the asymptotic values.

Detecting a jet transition at optical wavelengths may be difficult if it occurs on

timescales of a week or more. In these cases the afterglow is weak and the light from the host galaxy may start to dominate the light curve (*e.g.*, Halpern et al. 2000). In such instances radio observations may be required to clarify matters, since the radio flux is increasing prior to t_j and changes in the lightcurve evolution due to the jet break are easily detected. Indeed, the jet in GRB 970508, which was very well observed in the radio is not discernible in the optical data. In this case, Frail, Waxman & Kulkarni (2000) found a wide-angle jet with an opening angle of 30° and $t_j \sim 30$ days (but see Chevalier & Li 2000).

A *Jet* model with $t_j \approx 26$ days fits the data remarkably well (see Figure 1). The strongest point in favor of the *Jet* model is that it reproduces the broad maximum (~ 1 mJy) seen from 5 GHz to 22 GHz. We expect such a plateau at t_j as all light curves for $\nu_a < \nu \leq \nu_m$ reach their peak fluxes (with only a weak $\nu^{1/3}$ frequency dependence) before undergoing a slow decline. Most other models predict a strong frequency dependence in peak flux which is not seen in this case.

Knowing t_j and the density of the ambient medium n_0 from the model fit (Table 3) we can make a geometric correction to the total isotropic energy E_γ , as determined from either the observed γ -ray fluence or the total energy of the afterglow E_{52} , from the fit to the afterglow data (Sari *et al.* 1999, Livio & Waxman 2000). This approach gives values for the jet opening angle θ_j between 10° and 20° , which for a two-sided jet reduces the GRB energy to $\sim 10^{51}$ erg. The rapid lateral expansion of the jet also accelerates the transition to the non-relativistic regime, resulting in a change in the evolution of the light curves. Since this occurs on a timescale $t_{NR} \sim t_j \theta_j^{-2} \sim 350$ days (Waxman, Kulkarni & Frail 1998), we do not expect the non-relativistic transition to be important for our data.

There is some freedom in our choice of ν_c . We know that a cooling break (*i.e.*, $\Delta\alpha = -0.25$) is not apparent in the R band light curve on timescales of 2-10 days, so we searched for solutions with ν_c above or below this frequency. We found that physically consistent solutions (*i.e.*, with non-negative host fluxes, and $\epsilon_B < 1$) were only possible for values of ν_c below the optical band.

As part of the fitting process we also solved for the host flux density in the R and K bands and for any local dust obscuration, assuming an LMC-like extinction law. This yields $f_{host}(R)=1.1 \mu\text{Jy}$, $f_{host}(K)=1.7 \mu\text{Jy}$ and $A_V^{host}=0.4$ (in the host galaxy restframe). Klose *et al.* (2000b) argued for significant dust extinction with $A_V^{host}=0.96$. However, they likely overestimated A_V^{host} since they assumed a spherical fireball model and arbitrarily located ν_c above the optical band. Moreover, we find that there is some covariance between the values of A_V^{host} and p so that only with a global fit, in which p is constrained by the radio data as well as the optical data, we can solve for A_V^{host} in a self-consistent manner.

In view of the claims linking GRBs with the collapse of massive stars (Galama *et al.* 1998, Bloom *et al.* 1999, Reichart 1999, Piro *et al.* 2000), we considered a final model of a spherical explosion into a wind-blown circumburst medium (*Wind*: Chevalier & Li 1999, Li & Chevalier 1999). The *Wind* model (Figure 1) fits the data as well as the *Jet* model. In fact, the two models have sufficiently similar χ^2 to be indistinguishable. The close match between the temporal slopes of the late-time 8.46 GHz light curve and the early R band light curve (see §4) is a point in favor of the *Wind* model since a steeper decline is expected for a jet geometry. Our failure to distinguish between these two models can be blamed on the absence of radio measurements (particularly at millimeter wavelengths) at early times. The rapid rise of the flux density below ν_a and ν_m in the *Wind* model and the strong frequency dependence of the peak flux (see Figure 1), make such measurements advantageous (Panaitescu & Kumar 2000a). Moreover, in principle the *Wind* model can be distinguished from the other models by the fact that in this model ν_c is increasing with time ($\nu_c \propto t^{1/2}$). However, in this case since ν_c lies below the optical/IR bands, this behavior would be distinguishable only at late time when the host flux dominates over the OT. As before we solved for the host flux and any dust extinction, yielding $f_{host}(R)=0.9 \mu\text{Jy}$, $f_{host}(K)=1.3 \mu\text{Jy}$ and $A_V^{host}=0.3$. In our view further (and more sophisticated) model fits are not warranted by these data.

In summary, we find that the radio and optical/NIR observations of the afterglow emission from GRB 000418 can be fit by two different models. The close similarity between the results of the *Wind* and *Jet* models has been noted for other GRBs: GRB 970508 (Frail *et al.* (2000), Chevalier & Li 2000), GRB 980519 (Frail *et al.* 2000b, Chevalier & Li 1999), GRB 000301C (Berger *et al.* 2000, Li & Chevalier 2000), and GRB 991208 (Galama *et al.* 2000, Li & Chevalier 2000). The resolution of this conflict is important, since it goes to the core of the GRB progenitor issue. If the GRB progenitor is a massive star then there must be evidence for a density gradient in the afterglow light curves, reflecting the stellar mass loss that occurs throughout the star’s lifetime (Chevalier & Li 1999, Panaitescu & Kumar 2000a). At present, an unambiguous case for a GRB afterglow expanding into a wind has yet to be found. On the contrary, most afterglows are better fit by a jet expanding in a constant density medium (*e.g.*, Harrison *et al.* 1999, Halpern *et al.* 2000, Panaitescu & Kumar 2000b) and thus we are faced with a peculiar situation. While there is good evidence linking GRBs to the dusty, gas-rich environments favored by hypernova progenitors (Bloom, Kulkarni & Djorgovski 2000, Galama & Wijers 2000), the expected mass loss signature is absent (or at best ambiguous) in all afterglows studied to date.

A. Diercks is supported by a Millikan Fellowship at Caltech. GRB research at Caltech is supported by NSF and NASA grants (SRK, SGD, FAH). KH is grateful for Ulysses

support under JPL Contract 958056, and for NEAR support under NAG 5 9503.

REFERENCES

- Berger, E. *et al.* 2000, ApJ, 545, 56.
- Bessell, M. S. and Brett, J. M. 1988, PASP, 100, 1134.
- Bloom, J. S. *et al.* 1998, ApJ, 508, L21.
- Bloom, J. S., Kulkarni, S. R., and Djorgovski, S. G. 2000, submitted to AJ. astro-ph/0010176.
- Bloom, J. S. *et al.* 1999, Nature, 401, 453.
- Bloom, J. S. *et al.* 2000, GCN notice 661.
- Chevalier, R. A. and Li, Z. 2000, ApJ, 536, 195.
- Chevalier, R. A. and Li, Z.-Y. 1999, ApJ, 520, L29.
- Frail, D. A. *et al.* 2000a, ApJ, 538, L129.
- Frail, D. A. *et al.* 2000b, ApJ, 534, 559.
- Frail, D. A., Waxman, E., and Kulkarni, S. R. 2000, ApJ, 537, 191.
- Fukugita, M., Shimasaku, K., and Ichikawa, T. 1995, PASP, 107, 945.
- Galama, T. J. *et al.* 2000, ApJ, 541, L45.
- Galama, T. J. *et al.* 1998, Nature, 395, 670.
- Galama, T. J. and Wijers, R. A. M. J. 2000, ApJ in press; astro-ph/0009367.
- Goodman, J. 1997, New Astr., 2(5), 449.
- Granot, J., Piran, T., and Sari, R. 1999a, ApJ, 513, 679.
- Granot, J., Piran, T., and Sari, R. 1999b, ApJ, 527, 236.
- Halpern, J. P. *et al.* 2000, ApJ, 543, 697.
- Harrison, F. A. *et al.* 1999, ApJ, 523, L121.

- Henden, A. 2000, GCN notice 662.
- Henden, A. *et al.* 2000, GCN notice 652.
- Hurley, K., Cline, T., and Mazets, E. 2000, GCN notice 642.
- Jorgensen, I. 1994, PASP, 106, 967.
- Klose, S. *et al.* 2000, ApJ, 545, 271.
- Klose, S. *et al.* 2000, GCN notice 645.
- Li, Z. and Chevalier, R. A. 1999, ApJ, 526, 716.
- Li, Z.-Y. and Chevalier, R. A. 2000, submitted to ApJ, astro-ph/0010288.
- Livio, M. and Waxman, E. 2000, ApJ, 538, 187.
- Mészáros, P. and Rees, M. J. 1997, ApJ, 476, 232.
- Metzger, M. R. and Fruchter, A. 2000, GCN notice 669.
- Mirabal, N., Halpern, J. P., and Wagner, R. M. 2000a, GCN notice 650.
- Mirabal, N., Halpern, J. P., and Wagner, R. M. 2000b, GCN notice 653.
- Mirabal, N. *et al.* 2000, GCN notice 646.
- Panaitescu, A. and Kumar, P. 2000a, ApJ, 543, 66.
- Panaitescu, A. and Kumar, P. 2000b, submitted to the ApJ, astro-ph/0010257.
- Piro, L. *et al.* 2000, Science, 290, 955.
- Reichart, D. E. 1999, ApJ, 521, L111.
- Rhoads, J. E. 1997, ApJ, 487, L1.
- Rhoads, J. E. 1999, ApJ, 525, 737.
- Sari, R., Piran, T., and Halpern, J. P. 1999, ApJ, 519, L17.
- Sari, R., Piran, T., and Narayan, R. 1998, ApJ, 497, L17.
- Schechter, P. L., Mateo, M., and Saha, A. 1993, PASP, 105, 1342.
- Schlegel, D. J., Finkbeiner, D. P., and Davis, M. 1998, ApJ, 500, 525.

- Taylor, J. H. and Cordes, J. M. 1993, *ApJ*, 411, 674.
- Tody, D. 1993, in *ASP Conf. Ser. 52: Astronomical Data Analysis Software and Systems II*, volume 2, 173+.
- Wade, R. A., Hoessel, J. G., Elias, J. H., and Huchra, J. P. 1979, *PASP*, 91, 35.
- Walker, M. A. 1998, *MNRAS*, 294, 307.
- Waxman, E. 1997, *ApJ*, 489, L33.
- Waxman, E., Kulkarni, S. R., and Frail, D. A. 1998, *ApJ*, 497, 288.
- Wijers, R. A. M. J. and Galama, T. J. 1999, *ApJ*, 523, 177.

Table 1. Optical/NIR Observations of GRB 000418

UT Date	Instr. ^a	Band	Mag. ^b	Err.	Ref. ^c
Apr 20.89	TNG 3.5m	R	21.54	0.04	2
Apr 20.90	CA 3.5m	K'	17.49	0.5	2
Apr 20.93	CA 1.2m	K'	17.89	0.2	2
Apr 21.15	MDM 2.4m	R	21.66	0.12	1
Apr 21.86	LO 1.5m	R	21.92	0.14	2
Apr 26.316	USNO 1.3m	R	22.65	0.20	2,4
Apr 27.26	MDM	R	22.77	0.23	1
Apr 28.170	P200	R	22.97	0.06	1
Apr 28.3	MDM	R	22.86	0.09	1
Apr 28.413	Keck/ESI	R	23.05	0.05	1
Apr 29.26	MDM	R	22.95	0.11	1
May 2.274	Keck/ESI	Gunn-i	23.38	0.05	1
May 2.28	MDM	R	23.19	0.12	1
May 2.285	Keck/ESI	B	24.31	0.08	1
May 2.31	USNO 1.3m	R	23.11	0.130	2
May 3.26	USNO 1.3m	R	23.41	0.160	2
May 4.44	UKIRT 3.8m	K	20.49	0.40	2
May 6.42	Keck/LRIS	R	23.48	0.10	7
May 8.89	TNG	R	23.30	0.05	2
May 8.92	TNG	V	23.92	0.07	2
May 9.82	USNO 1.0m	R	23.37	0.21	2
May 23.93	TNG	R	23.37	0.10	2
May 29.228	P200	R	23.66	0.15	1
Jun 2.88	CA 3.5m	R	23.32	0.08	2
Jun 2.91	TNG	R	23.57	0.05	2

^aCA 3.5m=Calar Alto 3.5-meter, USNO1.3m = U.S. Naval Observatory Flagstaff Station 1.3-meter, ESI=W.M. Keck Observatory Echellette Spectrograph-Imager, LRIS=W.M. Keck Observatory Low-Resolution Imaging Spectrograph

^bOptical photometry is on the Kron-Cousins and Gunn systems and referred to that of Henden (2000.) Data are corrected for Galactic extinction corresponding to $E(B - V) = 0.032$ derived from the maps of Schlegel *et al.* (1998).

^c1=this work, 2=Klose *et al.* 2000, 3=Mirabal *et al.* 2000, 4=Henden *et al.* 2000, 5=Mirabal, Halpern & Wagner 2000a, 6=Mirabal, Halpern & Wagner 2000b, 7=Metzger & Fruchter 2000

Table 2. Radio Observations of GRB 000418

Epoch (UT)	Telescope	ν_0 (GHz)	$S \pm \sigma$ (μJy)
2000 Apr 28.75	Ryle	15.0	550 \pm 600
2000 Apr 29.07	VLA	8.46	856 \pm 33
2000 Apr 30.07	VLA	8.46	795 \pm 37
2000 Apr 30.73	Ryle	15.0	1350 \pm 480
2000 May 1.06	VLA	4.86	110 \pm 52
2000 May 1.06	VLA	8.46	684 \pm 48
2000 May 2.93	Ryle	15.0	850 \pm 300
2000 May 3.04	VLA	4.86	1120 \pm 52
2000 May 3.04	VLA	8.46	1240 \pm 46
2000 May 3.04	VLA	22.46	1100 \pm 150
2000 May 4.97	VLA	1.43	210 \pm 180
2000 May 4.97	VLA	4.86	710 \pm 47
2000 May 4.97	VLA	8.46	1020 \pm 53
2000 May 4.97	VLA	22.46	860 \pm 141
2000 May 7.18	VLBA	8.35	625 \pm 60
2000 May 9.25	VLA	8.46	926 \pm 53
2000 May 16.13	VLA	8.46	963 \pm 34
2000 May 18.24	VLA	4.86	567 \pm 50
2000 May 18.24	VLA	8.46	660 \pm 50
2000 May 18.24	VLA	22.46	610 \pm 114
2000 May 22.21	VLA	8.46	643 \pm 38
2000 May 26.92	VLA	4.86	1105 \pm 51
2000 May 26.92	VLA	8.46	341 \pm 50
2000 Jun 1.14	VLA	8.46	556 \pm 43
2000 Jun 1.14	VLA	22.46	710 \pm 16
2000 Jun 3.04	VLA	8.46	517 \pm 34
2000 Jun 7.01	VLA	8.46	238 \pm 38
2000 Jun 11.93	VLA	8.46	230 \pm 33
2000 Jun 15.13	VLA	8.46	325 \pm 30
2000 Jun 20.10	VLA	8.46	316 \pm 30
2000 Jun 23.19	VLA	8.46	306 \pm 29
2000 Jun 27.08	VLA	8.46	296 \pm 22
2000 Jul 02.98	VLA	8.46	274 \pm 22
2000 Jul 10.04	VLA	8.46	178 \pm 24
2000 Jul 22.81	VLA	8.46	152 \pm 23
2000 Jul 22.81	VLA	4.86	192 \pm 25
2000 Jul 28.50	VLA	8.46	168 \pm 22
2000 Jul 28.50	VLA	4.86	191 \pm 25
2000 Aug 17.74	VLA	8.46	119 \pm 25
2000 Aug 17.74	VLA	4.86	235 \pm 31
2000 Aug 21.65	VLA	4.86	142 \pm 35

Table 2—Continued

Epoch (UT)	Telescope	ν_0 (GHz)	$S \pm \sigma$ (μJy)
2000 Aug 21.65	VLA	8.46	87 ± 31
2000 Aug 25.78	VLA	4.86	238 ± 34
2000 Aug 25.78	VLA	8.46	166 ± 27
2000 Aug 27.89	VLA	8.46	100 ± 25
2000 Sep 10.73	VLA	8.46	148 ± 25
2000 Sep 18.68	VLA	8.46	55 ± 20
2000 Sep 26.62	VLA	8.46	85 ± 22
2000 Nov 06.55	VLA	8.46	94 ± 14

Note. — The columns are (left to right), (1) UT date of the start of each observation, (2) telescope name, (3) observing frequency, and (4) peak flux density at the best fit position of the radio transient, with the error given as the root mean square noise on the image.

Table 3. Model parameters for GRB 000418

Parameters ^a	ISM	Jet	Wind
ν_a (Hz)	4.1×10^9	1.7×10^9	30×10^9
ν_m (Hz)	2.3×10^{11}	1.8×10^{10}	5.8×10^{11}
ν_c (Hz)	2×10^{15}	10^{14}	1.8×10^{13}
f_m (mJy)	2.5	3.4	10.4
p	2.3	2.4	2.2
t_{jet} (days)	—	25.7	—
A_V^{host}	0.0	0.4	0.3
χ^2/dof	326/54	165/54	184/54
E_{52}	11	10	4
n_0 or A^*	0.01	0.02	0.14
ϵ_B	0.05	0.06	0.04
ϵ_e	0.03	0.10	0.07

^aFor the *ISM* and *Wind* models ν_a , ν_m , ν_c and f_m are the self-absorption, synchrotron peak, and cooling frequencies, and the peak flux density, respectively on day 1. For the *Jet* model these values are referenced instead to the jet break time $t_j=25.7$ d. p is the electron power-law index and A_V is the V band extinction in the rest frame of the host galaxy ($z=1.118$), assuming an LMC-like extinction curve. Note that in the *Jet* and *ISM* models ν_c was fixed at 10^{14} and 2×10^{15} Hz, respectively, but in the *Wind* model it was left as a free parameter. The resulting values of χ^2 include an estimated contribution of interstellar scattering (ISS) and the increased error in subtracting off a host galaxy flux from each of the optical points. The model parameters are the total isotropic energy E_{52} in units of 10^{52} erg, the ambient density n_0 in cm^{-3} or in the case of the *Wind* model the parameter A^* as defined by Chevalier & Li (1999). ϵ_e and ϵ_B are the fraction of the shock energy in the electrons and the magnetic field, respectively. The true uncertainties in the derived parameters are difficult to quantify due to covariance, but we estimate that they range from 10 – 20%

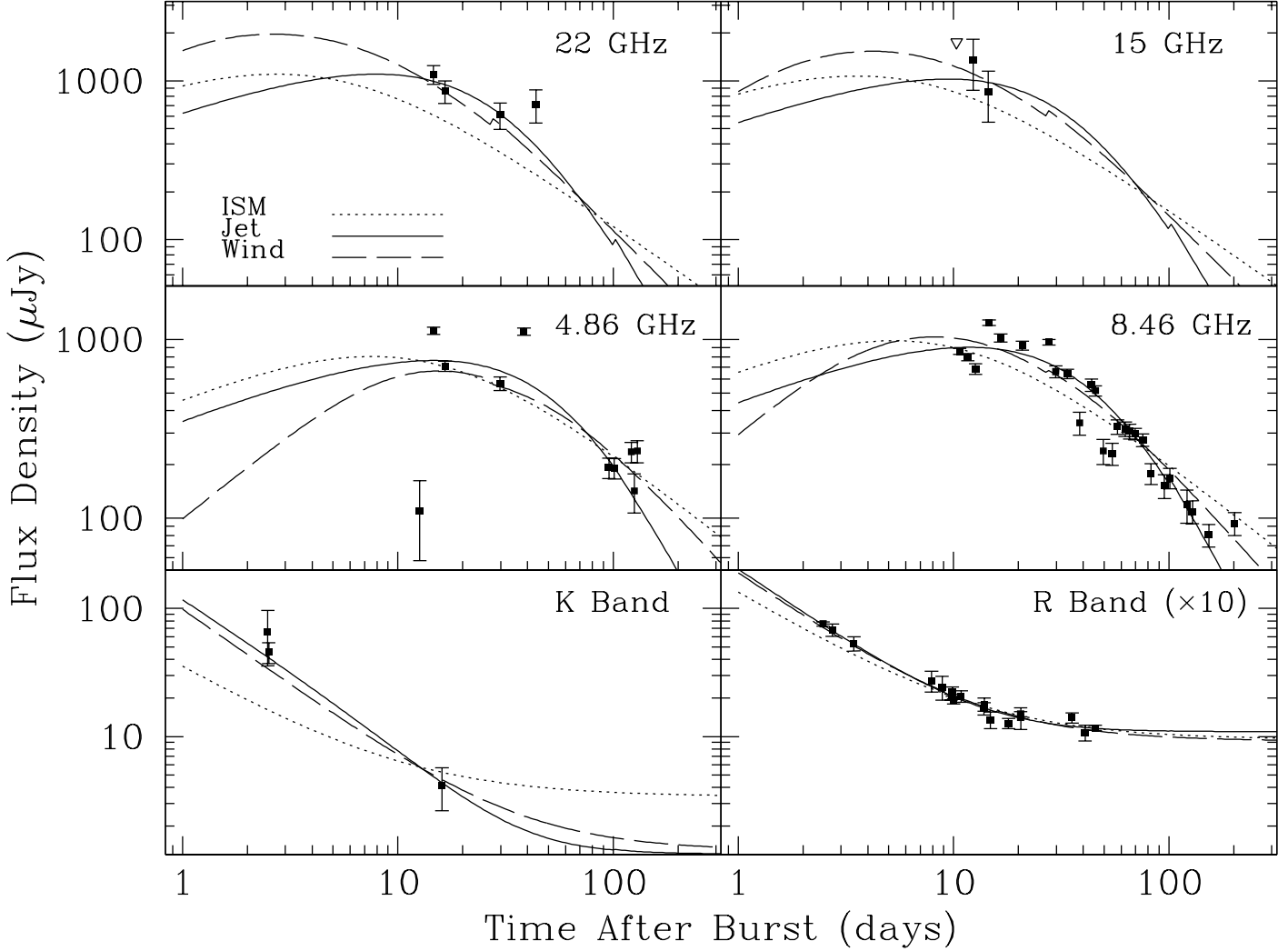


Fig. 1.— Radio and optical light curves for GRB000418. The observing frequency (or band) is shown in the upper right corner of each panel. Optical magnitudes were first corrected for Galactic foreground reddening before converting to flux units. For display purposes the R band flux densities have been increased by a factor of 10. The 8.46 GHz measurements on August 25 and September 18 are 3-epoch averages taken over a period of 7 days and 15 days, respectively. The dotted, solid and dashed lines are light curves for ISM, jet and wind models, respectively. They were derived from a global fit to the entire broad-band dataset. See text for more details.